# Conformational Profile of a Proline−Arginine Hybrid

Guillermo Revilla-López,[†] Ana I. Jiménez,[‡] Carlos Cativiela,[‡] Ruth Nussinov,[§,||] Carlos Alemán,*[,†,⊥] and David Zanuy*[,†]

Departament d'Enginyeria Química, E. T. S. d'Enginyeria Industrial de Barcelona, Universitat Politècnica de Catalunya, Diagonal 647, Barcelona E-08028, Spain, Departamento de Química Orgánica, Instituto de Ciencia de Materiales de Aragón, Universidad de Zaragoza−CSIC, 50009 Zaragoza, Spain, Basic Science Program, SAIC-Frederick, Inc. Center for Cancer Research Nanobiology Program, NCI, Frederick, Maryland 21702, Department of Human Genetics, Sackler Medical School, Tel Aviv University, Tel Aviv 69978, Israel, and Center for Research in Nano-Engineering, Universitat Politècnica de Catalunya, Campus Sud, Edifici C', C/Pasqual i Vila s/n, Barcelona E-08028, Spain

Received April 9, 2010

The intrinsic conformational preferences of a new nonproteinogenic amino acid have been explored by computational methods. This tailored molecule, named ($^{\beta}$Pro)Arg, is conceived as a replacement for arginine in bioactive peptides when the stabilization of folded turn-like conformations is required. The new residue features a proline skeleton that bears the guanidilated side chain of arginine at the C$^{\beta}$ position of the five-membered pyrrolidine ring, in either a cis or a trans orientation with respect to the carboxylic acid. The conformational profiles of the *N*-acetyl-*N*′-methylamide derivatives of the cis and trans isomers of ($^{\beta}$Pro)Arg have been examined in the gas phase and in solution by B3LYP/6-31+G(d,p) calculations and molecular dynamics simulations. The main conformational features of both isomers represent a balance between geometric restrictions imposed by the five-membered pyrrolidine ring and the ability of the guanidilated side chain to interact with the backbone through hydrogen bonds. Thus, both *cis*- and *trans*-($^{\beta}$Pro)Arg exhibit a preference for the $\alpha_L$ conformation as a consequence of the interactions established between the guanidinium moiety and the main-chain amide groups.

## INTRODUCTION

Design of specific chemical modifications in natural amino acids is a powerful strategy for controlling the conformational properties of short peptides.[1,2] Moreover, noncoded residues in a peptide chain can result in increased resistance to proteolytic degradation.[3−7] Nonproteinogenic amino acids are useful in engineering peptide analogues with improved pharmacokinetics and medicinal applications.[3−9]

A noncoded amino acid can replace residues in natural peptide sequences if it does not disrupt the bioactive conformation of the preplaced segment. The resulting peptide must preserve the native shape that interacts with the receptor. When dealing with small flexible peptides, a noncoded residue can improve the targeted peptide by biasing its conformational equilibrium to a conformational set that guarantees function. Thus, the nonproteinogenic amino acid should exhibit a high preference for the conformation adopted by the natural residue that is to be replaced.

Theoretical methods can assist in this effort so that only those candidates yielding satisfactory results in silico are selected for experimental studies. This evaluation requires (i) theoretical study of the wild-type bioactive conformation (if not available experimentally), (ii) assessment of which amino acid should be replaced, and (iii) design of a new noncoded amino acid adequate to replace the targeted position of the peptide. The conformational preferences of the new noncoded amino acid need to be determined before the replacement is performed. If such conformational preferences do not match those of the targeted position, the replacement will not be successful.

We are involved in a project aimed at improving the bioactivity of the pentapeptide Cys-Arg-Glu-Lys-Ala (CREKA). This peptide is of biotechnological interest because it recognizes molecular markers that are present in tumor blood vessels but not in the vasculature of normal tissues,[10] thus showing promising applications in cancer diagnosis and therapy. Medicinal use is hampered, however, by the poor stability against proteases and short half-life time typically exhibited by small and medium-sized natural peptides. The conformational landscape of CREKA has been explored by computational methods under different environmental conditions.[11] This analysis led to a bioactive conformation exhibiting a turn motif, with the charged side chains of Arg, Glu, and Lys oriented toward the same side of the molecule.[11] The peptide backbone is folded in a $\beta$-turn centered at the Arg and Glu residues. Arginine occupies the first corner position of the $\beta$-turn ($i + 1$) and adopts dihedral angles corresponding to the $\alpha$-helical ($\alpha_L$) region of the Ramachandran map.

The first attempt to decrease the peptide sensitivity to proteases was made by introducing unspecific chemical modifications that did not affect the overall conformational properties.[12] Hence, a methyl group replaced the hydrogen

* Corresponding authors e-mail: carlos.aleman@upc.edu (C.A.), david.zanuy@upc.edu (D.Z.).
[†] Universitat Politècnica de Catalunya.
[‡] Universidad de Zaragoza−CSIC.
[§] NCI.
[||] Tel Aviv University.
[⊥] Universitat Politècnica de Catalunya.

10.1021/ci100135f 
Published on Web 10/01/2010

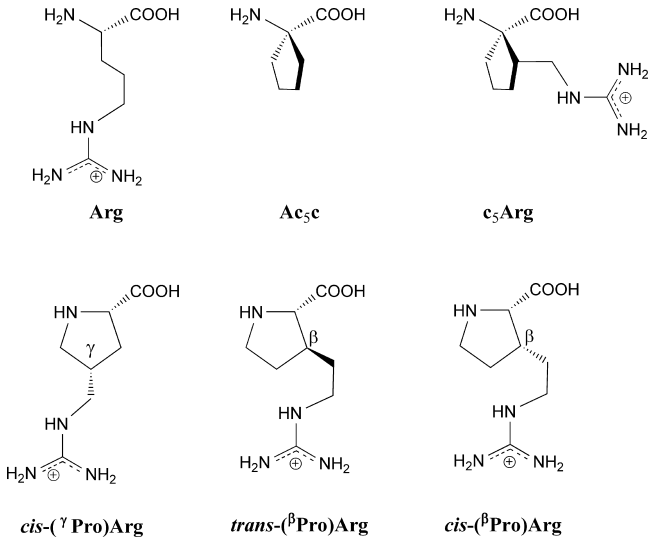


**Figure 1.** Structures of arginine (Arg) and some studied analogues. The first presented analogue was designed on 1-aminocyclopentane-1-carboxylic acid ($Ac_5c$), which led to the amino acid $c_5$Arg (ref 13) and those based on the proline structure (Pro): *cis*-($^{\gamma}$Pro)Arg (ref 28), *trans*-($^{\beta}$Pro)Arg, and *cis*-($^{\beta}$Pro)Arg, the last of which is the focus of this study. The arginine surrogates are named according to the $\gamma/\beta$ position of the proline skeleton bearing the guanidilated side chain and the trans/cis relative orientation between this side chain and the carboxylic acid.

atom at either the N position or the $C^{\alpha}$ position. This simple approach increased the in vivo half-life time of CREKA-coated nanoparticles in the tumor vessels.[12] Then, in a second stage, we undertook the design of new noncoded amino acids that could bias the folding of CREKA toward its bioactive organization, focusing our efforts on arginine surrogates. The main goal was to incorporate the side-chain functionality of arginine, which is essential for CREKA's activity, in a residue that presented clear conformational preferences for the $\alpha_L$ region of the Ramachandran map.

A first amino acid was designed by combining a noncoded amino acid of the family 1-aminocycloalkane-1-carboxylic acids ($Ac_nc$, where $n$ refers to the size of the cycle) and the side-chain functionality of arginine (Figure 1).[13] These amino acid series had been previously investigated and shown to exhibit a restricted conformational space characterized by a high propensity to adopt $\varphi,\psi$ backbone angles typical of the $3_{10}$-/α-helix (with some distortion in the case of $Ac_3c$).[14−18] The new amino acid (denoted as $c_5$Arg, Figure 1) was built by incorporating the side chain of arginine at the $\beta$-carbon atom of $Ac_5c$.[13] The intrinsic conformational preferences of the new amino acid were studied using theoretical methods, showing that the α-helical conformation was favored both in the gas phase and in solution. It was remarkable that the ability of the guanidinium moiety to form hydrogen bonds with the peptide backbone conditioned the conformational features of the parent $Ac_5c$,[17] which tends to favor the formation of $\gamma$-turns instead of α-helix-like arrangements.

The later challenge was to achieve similar results with a backbone constitution closer to that of coded amino acids. Among proteinogenic amino acids, proline is known to both impart protection against proteolytic cleavage[19−22] and nucleate peptide turns,[23−25] with a marked propensity to occupy the $i + 1$ position of $\beta$-turns. Accordingly, following the previous strategy, we generated a new residue by attaching the arginine side chain to the proline skeleton (see the Supporting Information for details). It should be noted that the cyclic nature of proline, which includes the amine nitrogen atom in the ring constitution, facilitates a cis arrangement of the peptide bond involving the pyrrolidine nitrogen, as compared to other peptide bonds, for which the cis form is almost nonexistent.[26,27] Here, however, this issue has not been addressed because the targeted arginine in wild-type CREKA presents both peptide bonds in the trans configuration[11] and the new residue is therefore useful only for the latter geometry.

In a previous work,[28] the guanidilated side chain was attached to the $\gamma$-carbon of the pyrrolidine ring in a cis configuration with the carboxylic acid moiety, thus giving rise to the residue denoted *cis*-($^{\gamma}$Pro)Arg in Figure 1. The chain length of this arginine analogue proved insufficient to reproduce the interactions observed for the guanidinium group in the bioactive conformation of CREKA.[11,28] Although the addition of another methylene unit to the exocyclic guanidilated substituent was favorable, incorporation of the resulting residue into CREKA led to the disruption of the $\beta$-turn conformation of the natural peptide.[28]

These results led us to design a new arginine surrogate built on a proline skeleton. Here, it is the $\beta$-pyrrolidine carbon that bears the guanidilated arginine side chain, and the resulting residue is termed *cis*-($^{\beta}$Pro)Arg, where cis refers to the position of the guanidilated substituent relative to the carboxylic acid and $\beta$ denotes the carbon atom of the five-membered ring where this substituent is placed (Figure 1). Prior to testing the modified pentapeptide Cys-*cis*($^{\beta}$Pro)Arg-Glu-Lys-Ala, the conformational propensities of the single amino acid have been investigated in depth by theoretical methods. As noted above, *cis*-($^{\beta}$Pro)Arg presents a cis orientation between the guanidinium and carbonyl moieties, as in the previously studied[28] *cis*-($^{\gamma}$Pro)Arg, in agreement with the spatial relationship characterized for the guanilidated segment of natural arginine in CREKA.[11] However, beyond the CREKA project, other peptides incorporating key arginine residues might present the guanidilated side chain oriented away form the carbonyl group in the bioactive form. This consideration prompted us to also evaluate in this work the conformational propensities of *trans*-($^{\beta}$Pro)Arg (Figure 1).

We have therefore performed quantum mechanics calculations on the *N*-acetyl-*N*′-methylamide derivatives of both *cis*-($^{\beta}$Pro)Arg and *trans*-($^{\beta}$Pro)Arg, hereafter denoted as Ac-*c*-($^{\beta}$Pro)Arg-NHMe and Ac-*t*-($^{\beta}$Pro)Arg-NHMe, respectively. The results are compared with those reported previously[28] for the analogous cis $\gamma$-substituted derivative, Ac-*c*-($^{\gamma}$Pro)Arg-NHMe. Additionally, we carried out the parametrization of the two nonproteinogenic amino acids under study before analyzing the conformational impact derived from their incorporation into biologically active peptides. The dynamical conformational features of the two residues have been explored in aqueous solution at room temperature using classical molecular dynamics (MD) simulations with explicit water molecules.

## COMPUTATIONAL METHODS

**Quantum Mechanical Calculations.** Density functional theory (DFT) methods were applied for quantum mechanical calculations, which were performed using the Gaussian 03

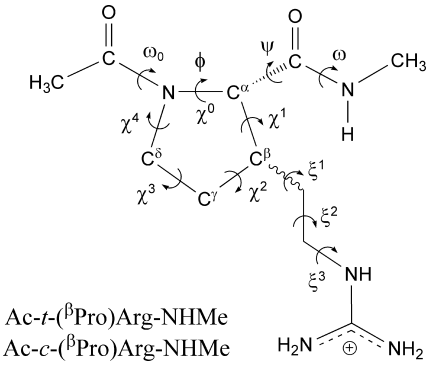


**Figure 2.** Dihedral angles used to identify the conformations of the *N*-acetyl-*N*′-methylamide derivatives of *trans*-($^{\beta}$Pro)Arg and *cis*-($^{\beta}$Pro)Arg studied in this work. The ($\varphi$,$\psi$) dihedral angles are defined by the atoms in the backbone, whereas the side-chain dihedral angles $\chi^i$ and $\xi^i$ are given by the pyrrolidine atoms and the exocyclic side-chain atoms, respectively. In particular, $\varphi$ and $\chi^0$ are defined as C(O)−N−C$^{\alpha}$−C(O) and C$^{\delta}$−N−C$^{\alpha}$−C$^{\beta}$, respectively. The dihedral angle $\xi^1$ is given by C$^{\alpha}$−C$^{\beta}$−C(H$_2$)−C(H$_2$).

computer program.[29] Specifically, calculations were carried out by combining the unrestricted formalism of the B3LYP functional[30,31] with the 6-31+G(d,p) basis set.[32] Frequency analyses were carried out to verify the nature of the minimum state of all of the stationary points obtained and to calculate the zero-point vibrational energies (ZPVEs) and both thermal and entropic corrections. These statistical terms were then used to compute the conformational Gibbs free energies in the gas phase ($\Delta G^{gp}$) at 298 K.

Figure 2 shows the backbone ($\omega_0$, $\varphi$, $\psi$, $\omega$) and side-chain ($\chi^i$, $\xi^i$) dihedral angles that define the conformations adopted by Ac-*t*-($^{\beta}$Pro)Arg-NHMe and Ac-*c*-($^{\beta}$Pro)Arg-NHMe. The minimum-energy structures characterized for these compounds are denoted using a three-label code that specifies the arrangement of the peptide backbone, the puckering of the five-membered cycle, and the conformation adopted by the exocyclic substituent. The first label identifies the backbone conformation type according to Perczel et al.'s nomenclature,[33] which categorizes the potential energy surface $E = E(\varphi,\psi)$ of α-amino acids in nine different regions: $\gamma_D$, $\delta_D$, $\alpha_D$, $\varepsilon_D$, $\beta_{DL}$, $\varepsilon_L$, $\alpha_L$, $\delta_L$, and $\gamma_L$. The presence of the pyrrolidine ring in proline fixes the $\varphi$ angle near −60°, and accordingly, only three such regions can be accessed,[23,24] namely, $\gamma_L$ ($\gamma$-turn), $\alpha_L$ (α-helix), and $\varepsilon_L$ (polyproline II). Identical geometric restrictions should apply to the arginine surrogates under study because they have a proline skeleton. A trans configuration was considered for the amide bonds ($\omega_0$, $\omega \approx 180°$). The second label describes the down [d] or up [u] puckering of the five-membered pyrrolidine ring.[23,34,35] Such conformational states are also called C$^{\gamma}_{endo}$ and C$^{\gamma}_{exo}$, respectively, and correspond to those in which the C$^{\gamma}$ atom and the carbonyl group of proline (or the proline-like residue) lie on the same and opposite sides of the plane defined by C$^{\delta}$, N, and C$^{\alpha}$. Specifically, a down puckering was assigned when $\chi^1$ and $\chi^3$ were positive and $\chi^2$ and $\chi^4$ were negative. Conversely, negative values of $\chi^1$ and $\chi^3$ and positive values of $\chi^2$ and $\chi^4$ correspond to an up-puckered pyrrolidine ring. Finally, the orientation of the polar exocyclic substituent is described by the third label, which indicates the gauche$^+$ (g$^+$), skew$^+$ (s$^+$), trans (t), skew$^-$ (s$^-$), gauche$^-$ (g$^-$), or cis (c) state of each $\xi^i$ dihedral angle.

The conformational search was performed following the strategy used in our previous work on *cis*-($^{\gamma}$Pro)Arg.[28] It was assumed that the two ($^{\beta}$Pro)Arg derivatives under study maintain the geometric restrictions derived from the cyclic nature of proline. Thus, the three minimum-energy conformations characterized[36] for Ac-Pro-NHMe with trans amide bonds, namely, $\gamma_L$[d], $\gamma_L$[u], and $\alpha_L$[u], were considered as starting geometries for Ac-*t*-($^{\beta}$Pro)Arg-NHMe and Ac-*c*-($^{\beta}$Pro)Arg-NHMe in the present work. Regarding the substituent attached to the $\beta$-carbon of the pyrrolidine moiety, each $\xi^i$ dihedral was expected to exhibit minima of the gauche$^+$, trans, and gauche$^-$ types. Accordingly, 3 (minima of Ac-Pro-NHMe[36]) × 3 (minima of $\xi^1$) × 3 (minima of $\xi^2$) × 3 (minima of $\xi^3$) = 81 minima were anticipated for the potential energy hypersurface $E = E(\varphi, \psi, \chi^i, \xi^i)$ of each ($^{\beta}$Pro)Arg derivative. All of these structures were used as starting points for subsequent full geometry optimizations.

The influence of the solvent on the conformational preferences of the compounds under study was quantified by performing self-consistent reaction field (SCRF) calculations on the optimized geometries. Under this formalism, the solute is treated at the quantum mechanical level, whereas the solvent is represented as a dielectric continuum. In particular, we used the polarizable continuum model (PCM) developed by Tomasi and co-workers to describe the bulk solvent.[37−40] PCM calculations were performed following the standard protocol and considering the dielectric constants of carbon tetrachloride ($\varepsilon = 2.228$), chloroform ($\varepsilon = 4.9$), and water ($\varepsilon = 78.4$). The conformational free energies in solution ($\Delta G^{sol}$, where sol refers to the solvent) were computed using the classical thermodynamics scheme; that is, for each minimum, the free energy of solvation provided by the PCM model was added to the $\Delta G^{gp}$ value.

**Force-Field Parametrization.** The stretching, bending, torsion, and van der Waals interactions of *trans*-($^{\beta}$Pro)Arg and *cis*-($^{\beta}$Pro)Arg were described classically by extrapolating the force-field parameters contained in the AMBER libraries[41] for proline and arginine. For selected minimum-energy conformations, electrostatic atomic-centered charges were calculated by fitting the UHF/6-31G(d) quantum mechanical and the Coulombic molecular electrostatic potentials (MEPs) to a large set of points placed outside the nuclear region. The electrostatic parameters derived at this level of theory are fully compatible with the current parameters of the AMBER force field.[41] Electrostatic force-field parameters for the two ($^{\beta}$Pro)Arg isomers were obtained by applying to such atomic charges a strategy based on a Boltzmann distribution of multiple conformations, which was originally proposed by different authors[42−44] and has been shown to be especially suitable for nonproteinogenic residues.[13,16,17,43,45] Moreover, this strategy provides conformationally independent electrostatic parameters.

**Force-Field Calculations.** MD simulations in water solution were performed using the NAMD program.[46] The Ac-*t*-($^{\beta}$Pro)Arg-NHMe or Ac-*c*-($^{\beta}$Pro)Arg-NHMe molecules were placed in the center of a cubic simulation box ($a$ = 30.6 Å) filled with 955 explicit water molecules, which were represented using the TIP3 model.[47] Negatively charged chloride atoms were added to reach electron neutrality. Before the production runs, the simulation box was equilibrated for each compound. Thus, 0.5 ns of *NVT*-MD at 500 K was used to homogeneously distribute the solvent and ions in the box. Next, 0.5 ns of *NVT*-MD at 298 K (thermal equilibration) and 0.5 ns of *NPT*-MD at 298 K (density

**Table 1.** Dihedral Angles (See Figure 2; in Degrees), Pseudorotational Parameters of the Pyrrolidine Ring (*A*, *P*; in Degrees), and Relative Energies ($\Delta E^{gp}$; in kcal/mol) of the Minimum-Energy Conformations with $\Delta E^{gp} < 5.0$ kcal/mol Characterized for Ac-*t*-($^{\beta}$Pro)Arg-NHMe at the B3LYP/6-31+G(d,p) Level

| conformer | $\omega_0$ | $\varphi$ | $\psi$ | $\omega$ | *A*, *P*[a] | $\xi^1$ | $\xi^2$ | $\xi^3$ | $\Delta E^{gp}$ |
|---|---|---|---|---|---|---|---|---|---|
| $\gamma_L$[u]s$^-$g$^+$t | −169.6 | −77.8 | 54.8 | 178.2 | 40.1, 92.5[b] | −127.0 | 61.1 | 162.8 | 0.0[c] |
| $\gamma_L$[u]g$^-$g$^-$s$^+$ | −170.3 | −79.9 | 59.5 | 179.1 | 39.0, 98.3[d] | −84.2 | −77.5 | 117.9 | 1.1 |
| $\gamma_L$[u]g$^-$g$^-$s$^-$ | −170.3 | −80.5 | 56.1 | 179.3 | 38.0, 103.3[e] | −59.8 | −49.6 | −115.6 | 1.5 |
| $\alpha_L$[u]s$^-$g$^+$t | −169.7 | −89.7 | −3.5 | 176.5 | 36.0, 112.0[f] | −92.4 | 61.2 | 156.5 | 2.1 |
| $\alpha_L$[u]g$^+$g$^-$t | −170.2 | −73.1 | −20.2 | 179.0 | 40.5, 76.2[g] | 39.5 | −77.7 | −173.7 | 3.0 |
| $\alpha_L$[u]g$^-$tg$^-$ | −169.9 | −76.5 | −16.0 | 177.2 | 38.0, 85.5[h] | −88.4 | 155.2 | −86.1 | 3.5 |
| $\gamma_L$[u]s$^-$tg$^-$ | −169.4 | −73.5 | 44.0 | 177.3 | 40.8, 85.5[i] | −126.2 | 157.4 | −87.1 | 3.7 |

[a] See ref 36 for definition. [b] $\chi^0 = -1.7°$, $\chi^1 = -22.3°$, $\chi^2 = 37.5°$, $\chi^3 = -38.2°$, $\chi^4 = 25.2°$. [c] $E = -856.5567162$ au. [d] $\chi^0 = -5.7°$, $\chi^1 = -18.4°$, $\chi^2 = 34.9°$, $\chi^3 = -38.0°$, $\chi^4 = 27.5°$. [e] $\chi^0 = -8.7°$, $\chi^1 = -15.1°$, $\chi^2 = 32.5°$, $\chi^3 = -37.3°$, $\chi^4 = 29.1°$. [f] $\chi^0 = -13.5°$, $\chi^1 = -9.2°$, $\chi^2 = 27.4°$, $\chi^3 = -35.4°$, $\chi^4 = 30.7°$. [g] $\chi^0 = 9.7°$, $\chi^1 = -30.7°$, $\chi^2 = 40.2°$, $\chi^3 = -34.5°$, $\chi^4 = 15.5°$. [h] $\chi^0 = 3.0°$, $\chi^1 = -24.6°$, $\chi^2 = 36.8°$, $\chi^3 = -35.1°$, $\chi^4 = 20.0°$. [i] $\chi^0 = 3.2°$, $\chi^1 = -26.6°$, $\chi^2 = 39.6°$, $\chi^3 = -37.4°$, $\chi^4 = 21.5°$.

relaxation) were carried out. The last snapshot of the *NPT*-MD run was used as the starting point for production *NVT*-MD runs at standard conditions.

The energy was calculated using the AMBER potential.[41] Atom-pair distance cut-offs were applied at 12.0 Å to compute the van der Waals and electrostatic interactions. To avoid discontinuities in the potential energy function, nonbonding energy terms were slowly converged to 0 by applying a smoothing factor from a distance of 10.0 Å. Both temperature and pressure were controlled using the weak coupling method[48] applying a time constant for heat-bath coupling and a pressure relaxation time of 1 ps. Bond lengths were constrained using the SHAKE algorithm[49] with a numerical integration step of 2 fs.

## RESULTS AND DISCUSSION

A total of 21 minimum-energy conformations were found and characterized for Ac-*t*-($^{\beta}$Pro)Arg-NHMe in the gas phase. The conformational parameters of those with relative energies ($\Delta E^{gp}$) below 5.0 kcal/mol are listed in Table 1 (the complete list is provided in the Supporting Information). In the global minimum ($\gamma_L$[u]s$^-$g$^+$t, Figure 3a), the terminal acetyl CO and methylamide NH groups are linked by a hydrogen bond ($d_{H\cdots O} = 1.793$ Å, $\angle N-H\cdots O = 151.3°$) closing a seven-membered cycle ($\gamma$-turn or $C_7$ conformation), and the pyrrolidine ring adopts an up puckering. The orientation of the exocyclic guanidilated side chain, which is defined by the skew$^-$, gauche$^+$, and trans arrangements of $\xi^1$, $\xi^2$ and $\xi^3$, respectively, enables the formation of a strong hydrogen bond between the carbonyl oxygen of the *trans*-($^{\beta}$Pro)Arg residue and the guanidinium NH site ($d_{H\cdots O} = 1.628$ Å, $\angle N-H\cdots O = 176.2°$). The second ($\gamma_L$[u]g$^-$g$^-$s$^+$, Figure 3b) and third ($\gamma_L$[u]g$^-$g$^-$s$^-$, Figure 3c) minima also exhibit the seven-membered hydrogen-bonded ring typical of a $C_7$ conformation and an up-puckered pyrrolidine moiety, but they differ from the global minimum in the orientation of the guanidilated side chain. In the $\gamma_L$[u]g$^-$g$^-$s$^+$ conformer, the side-chain···backbone interaction involves an $NH_2$ group in the guanidinium substituent instead of the NH site. The less favorable arrangement of the exocyclic side chain in these two conformers produces a destabilization of 1.1−1.5 kcal/mol with respect to the global minimum. A similar but more pronounced effect is observed for the last minimum listed in Table 1 ($\gamma_L$[u]s$^-$tg$^-$, Figure 3g). This conformer presents shapes for both the peptide backbone and the pyrrolidine moiety that are identical to those described above for the first, second, and third minima, but a much higher energy ($\Delta E^{gp} = 3.7$ kcal/mol). This destabilization should be attributed to the unfavorable steric interactions produced within the methylene groups in the side chain to allow the formation of a hydrogen bond between the *trans*-($^{\beta}$Pro)Arg CO and the guanidinium $NH_2$.

The most stable structure in Table 1 exhibiting a backbone conformation other than a $\gamma$-turn is $\alpha_L$[u]s$^-$g$^+$t, which is unfavored by 2.1 kcal/mol with respect to the global minimum. This is noteworthy, because the most stable $\alpha_L$ conformation with trans amide bonds characterized for Ac-Pro-NHMe exhibits a $\Delta E^{gp}$ value of 4.9 kcal/mol.[36] The $\alpha_L$[u]s$^-$g$^+$t minimum of Ac-*t*-($^{\beta}$Pro)Arg-NHMe (Figure 3d) presents no hydrogen-bonding interaction within the backbone amide groups, but is stabilized by a strong backbone··· side-chain hydrogen bond. The two additional $\alpha_L$ conformers in Table 1, $\alpha_L$[u]g$^+$g$^-$t (Figure 3e) and $\alpha_L$[u]g$^-$tg$^-$ (Figure 3f), exhibit similar arrangements for the peptide backbone and the pyrrolidine ring while differing in the orientation of the guanidilated substituent and the topology of the associated backbone···side-chain interaction. Local repulsions within the aliphatic segment in this exocyclic side chain produce a destabilization of 0.9 and 1.4 kcal/mol, respectively, relative to the most stable $\alpha_L$ conformer.

Comparison with the results reported previously[28] for Ac-*c*-($^{\gamma}$Pro)Arg-NHMe provides evidence for the higher flexibility of the $\beta$-substituted derivative Ac-*t*-($^{\beta}$Pro)Arg-NHMe studied in the present work. This is due to the presence of an additional exocyclic methylene unit in the latter case (Figure 1), which broadens the conformational space that can be explored by the guanidilated side chain. Yet, the number of energetically accessible conformers is small in both cases, as expected from the restrictions imposed by the proline skeleton. The two compounds share the main structural features of the global minimum, which belongs to the $\gamma_L$[u] category and exhibits identical patterns for both the backbone···backbone and side-chain···backbone hydrogen-bonding interactions. However, a highly stable $\gamma_L$[d] conformer was located[28] for Ac-*c*-($^{\gamma}$Pro)Arg-NHMe at only 0.4 kcal/mol, whereas no $\gamma_L$[d] structure appears in Table 1 for Ac-*t*-($^{\beta}$Pro)Arg-NHMe. Indeed, the only $\gamma_L$[d] minimum located for the latter compound presents $\Delta E^{gp} = 19.0$ kcal/mol (see the Supporting Information). Another important difference is the presence of $\alpha_L$ conformers in Table 1, whereas no Ac-*c*-($^{\gamma}$Pro)Arg-NHMe minima[28] presented this backbone conformation.

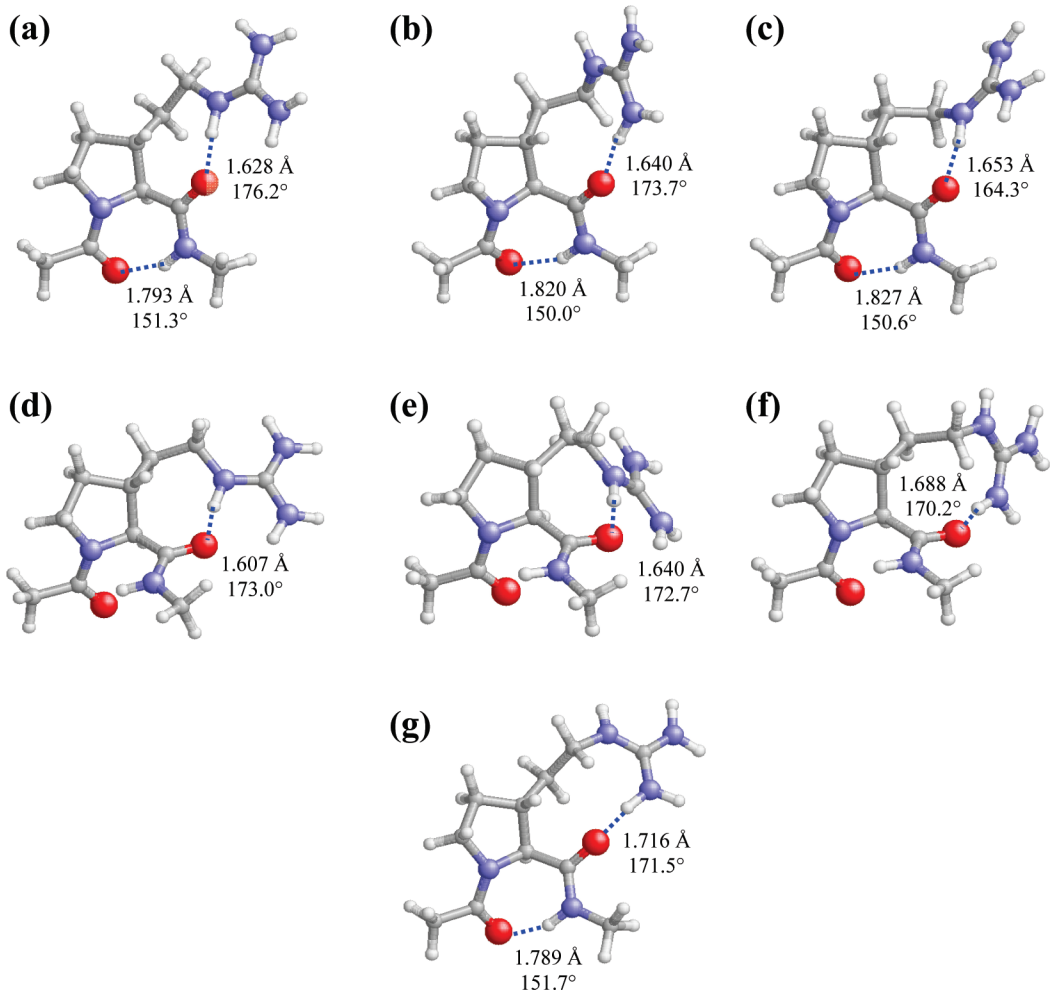


**Figure 3.** Selected minimum-energy conformations of Ac-*t*-($^{\beta}$Pro)Arg-NHMe obtained from B3LYP/6-31+G(d,p) calculations ($\Delta E^{gp} < 5.0$ kcal/mol; see Table 1): (a) $\gamma_L$[u]s$^-$g$^+$t, (b) $\gamma_L$[u]g$^-$g$^-$s$^+$, (c) $\gamma_L$[u]g$^-$g$^-$s$^-$, (d) $\alpha_L$[u]s$^-$g$^+$t, (e) $\alpha_L$[u]g$^+$g$^-$t, (f) $\alpha_L$[u]g$^-$tg$^-$, and (g) $\gamma_L$[u]s$^-$tg$^-$. Intramolecular hydrogen bonds are indicated by dashed lines (H···O distances and N−H···O angles are given).

**Table 2.** Dihedral Angles (See Figure 2; in Degrees), Pseudorotational Parameters of the Pyrrolidine Ring (*A*, *P*; in Degrees), and Relative Energies ($\Delta E^{gp}$; in kcal/mol) of the Minimum-Energy Conformations with $\Delta E^{gp} < 5.0$ kcal/mol Characterized for Ac-*c*-($^{\beta}$Pro)Arg-NHMe at the B3LYP/6-31+G(d,p) Level

| conformer | $\omega_0$ | $\varphi$ | $\psi$ | $\omega$ | *A*, *P*[a] | $\xi^1$ | $\xi^2$ | $\xi^3$ | $\Delta E^{gp}$ |
|---|---|---|---|---|---|---|---|---|---|
| $\alpha_L$[d]g$^+$g$^-$t | −169.7 | −86.3 | −11.6 | 175.3 | 39.6, −108.3[b] | 75.3 | −71.4 | 178.9 | 0.0[c] |
| $\alpha_L$[d]g$^+$ts$^+$ | −169.2 | −90.1 | −4.3 | 174.5 | 40.1, −111.7[d] | 69.2 | −172.0 | 95.2 | 1.3 |
| $\gamma_L$[d]s$^-$g$^+$t | −171.1 | −84.1 | 75.5 | −176.7 | 39.8, −117.0[e] | −116.3 | 70.4 | 164.2 | 2.0 |
| $\gamma_L$[d]s$^-$ts$^-$ | −170.3 | −83.1 | 66.4 | −178.5 | 40.0, −113.6[f] | −104.8 | 168.1 | −93.4 | 3.1 |
| $\gamma_L$[u]s$^+$g$^-$t | −168.7 | −66.8 | 31.8 | 174.5 | 43.7, 78.2[g] | 127.7 | −65.4 | 178.3 | 3.9 |

[a] See ref 36 for definition. [b] $\chi^0 = -12.4°$, $\chi^1 = 31.7°$, $\chi^2 = -39.6°$, $\chi^3 = 32.0°$, $\chi^4 = -12.2°$. [c] $E = -856.554209$ au. [d] $\chi^0 = -14.8°$, $\chi^1 = 33.5°$, $\chi^2 = -40.1°$, $\chi^3 = 31.0°$, $\chi^4 = -10.0°$. [e] $\chi^0 = -18.1°$, $\chi^1 = 35.0°$, $\chi^2 = -39.5°$, $\chi^3 = 28.3°$, $\chi^4 = -6.3°$. [f] $\chi^0 = -16.0°$, $\chi^1 = 34.1°$, $\chi^2 = -40.0°$, $\chi^3 = 30.0°$, $\chi^4 = -8.8°$. [g] $\chi^0 = 8.9°$, $\chi^1 = -32.1°$, $\chi^2 = 43.4°$, $\chi^3 = -38.2°$, $\chi^4 = 18.1°$.

Table 2 gives the conformational parameters of the five minima characterized for Ac-*c*-($^{\beta}$Pro)Arg-NHMe with $\Delta E^{gp}$ values below 5.0 kcal/mol (see the Supporting Information for a complete list of minima). Interestingly, the backbone shape preferred by this compound corresponds to the α-helix, whereas the γ-turn is unfavored by at least 2.0 kcal/mol. This is in sharp contrast with the result described above for the *trans*-($^{\beta}$Pro)Arg derivative, as well as with the behavior observed before for the analogous γ-substituted compound[28] [Ac-*c*-($^{\gamma}$Pro)Arg-NHMe] and for proline itself[36] (Ac-Pro-NHMe). Indeed, the most stable α-helical minimum characterized for Ac-Pro-NHMe with trans amide bonds lies 4.9 kcal/mol above the preferred γ-turn conformer,[36] and no minimum-energy structure was characterized in the α-helix region for Ac-*c*-($^{\gamma}$Pro)Arg-NHMe.[28] This comparative analysis provides evidence for the enormous impact that the incorporation of a functionalized side chain that is able to establish hydrogen-bonding interactions with the main-chain amide groups can have on the conformational preferences of the peptide backbone. It also illustrates the fact that the conformational profile of arginine analogues bearing a proline skeleton depends dramatically on the specific position of the guanidilated side chain, that is, the pyrrolidine carbon bearing it and its relative orientation with respect to the carboxyl terminus.

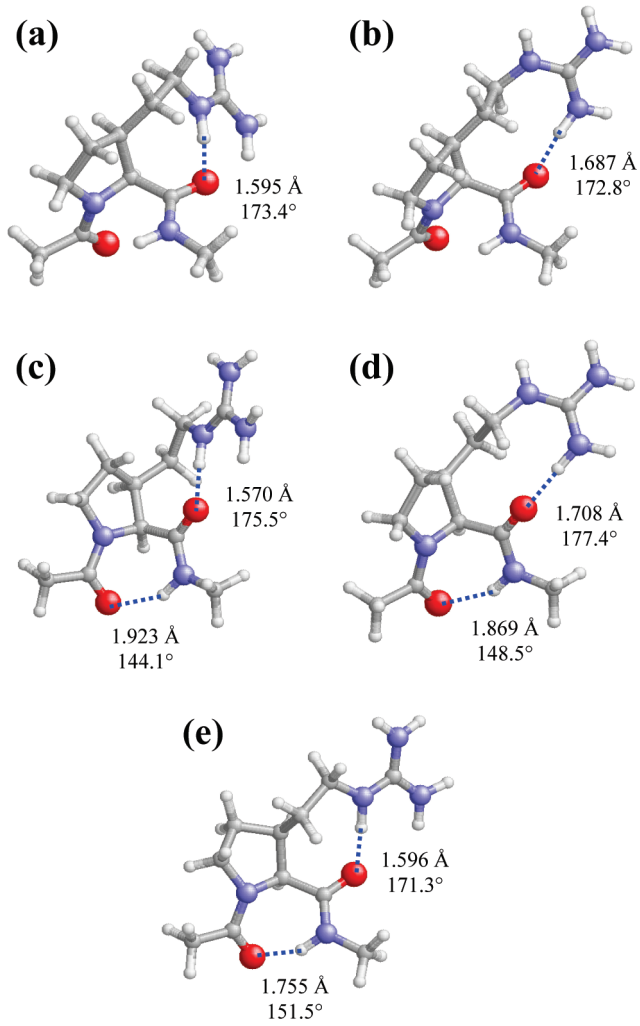


**Figure 4.** Selected minimum-energy conformations of Ac-*c*-($^{\beta}$Pro)Arg-NHMe obtained from B3LYP/6-31+G(d,p) calculations ($\Delta E^{gp} < 5.0$ kcal/mol; see Table 2): (a) $\alpha_L$[d]g$^+$g$^-$t, (b) $\alpha_L$[d]g$^+$ts$^+$, (c) $\gamma_L$[d]s$^-$g$^+$t, (d) $\gamma_L$[d]s$^-$ts$^-$, and (e) $\gamma_L$[u]s$^+$g$^-$t. Intramolecular hydrogen bonds are indicated by dashed lines (H···O distances and N−H···O angles are given).

As expected for an α-helical conformer, the lowest-energy minimum of Ac-*c*-($^{\beta}$Pro)Arg-NHMe ($\alpha_L$[d]g$^+$g$^-$t, Figure 4a) exhibits no hydrogen-bonding interaction involving the backbone amide groups. However, a very strong hydrogen bond is established between the *cis*-($^{\beta}$Pro)Arg CO and guanidinium NH sites ($d_{H\cdots O}$ = 1.595 Å, ∠N−H···O = 173.4°). The $\alpha_L$ backbone conformation and the down pyrrolidine puckering are also present in the second minimum ($\alpha_L$[d]g$^+$ts$^+$, Figure 4b). However, the less favorable backbone···side-chain interaction in this case, which involves a guanidinium $NH_2$ moiety, produces a destabilization of 1.3 kcal/mol.

The remaining Ac-*c*-($^{\beta}$Pro)Arg-NHMe minima in Table 2 exhibit a γ-turn conformation stabilized by the corresponding hydrogen bond connecting the acetyl CO and methylamide NH groups. The two most stable conformers of this type, $\gamma_L$[d]s$^-$g$^+$t (Figure 4c) and $\gamma_L$[d]s$^-$ts$^-$ (Figure 4d), retain the down pyrrolidine puckering observed in the helical minima and differ from each other in the guanidinium site ($NH/NH_2$) that is hydrogen-bonded to the carbonyl group of *cis*-($^{\beta}$Pro)Arg. Comparison of their relative energies (2.0 and 3.1 kcal/mol, respectively) suggests that the guanidinium NH provides a better geometry for hydrogen bonding to the main chain and therefore produces a higher stabilizing effect, as observed before for the helical conformers (Figure 4a,b). It should be noted that the most stable $\alpha_L$ and $\gamma_L$ conformers characterized for the *trans*-($^{\beta}$Pro)Arg derivative (Table 1) also present backbone···side-chain interactions involving the NH guanidinium site. Therefore, this seems to be a general trend of ($^{\beta}$Pro)Arg, independently of the cis/trans relative orientation of the guanidilated side chain.

The *trans*-($^{\beta}$Pro)Arg and *cis*-($^{\beta}$Pro)Arg derivatives investigated in this work differ not only in their respective preferences to accommodate γ-turn or α-helical backbone arrangements. These compounds also exhibit different conformational propensities in their five-membered ring. Thus, all minima in Table 1 exhibit an up-puckered pyrrolidine unit, whereas the most stable Ac-*c*-($^{\beta}$Pro)Arg-NHMe minima (Table 2) present a down puckering. Moreover, the preference for a particular arrangement of the five-membered ring is much more pronounced in the former case, as evidenced by the fact that the first up-puckered minimum of *cis*-($^{\beta}$Pro)Arg lies 3.9 kcal/mol above the global minimum (Table 2) whereas no minimum exhibiting a conformation other than up was identified below 7.0 kcal/mol for the trans isomer (see the Supporting Information). Indeed, arrangements of the pyrrolidine ring rarely observed in proline and proline-like residues were found to be preferred over the down conformation for this compound (see the Supporting Information). The contrast between the puckering tendencies of the five-membered ring in *trans*-($^{\beta}$Pro)Arg and *cis*-($^{\beta}$Pro)Arg becomes most evident when minima in the $\gamma_L$ region are compared. Thus, for the cis isomer (Table 2), the most stable $\gamma_L$[d] and $\gamma_L$[u] minima are separated by an energy gap of only 1.9 kcal/mol, whereas the corresponding energy difference for the trans derivative amounts to 19.0 kcal/mol (Table 1 and Supporting Information). This distinct behavior should be ascribed to the different spatial relative dispositions between the ($^{\beta}$Pro)Arg carbonyl and guanidinium groups in the compounds under study. In both cases, the pyrrolidine puckering providing optimal geometry for the establishment of hydrogen-bonding interactions between the two groups mentioned is preferred. For *cis*-($^{\beta}$Pro)Arg, both substituents lie on the same face of the five-membered cycle and are therefore close enough to interact for any puckering state. In contrast, the two interacting groups exhibit a trans relative orientation in *trans*-($^{\beta}$Pro)Arg, and it is the up (but not the down) arrangement of the pyrrolidine ring that brings them into close proximity, thus allowing for strong hydrogen bonding. For the trans isomer, the up puckering is particularly favorable in the case of $\gamma_L$ conformers, because positive $\psi$ values make the carbonyl oxygen of *trans*-($^{\beta}$Pro)Arg point in the opposite direction to where the guanidilated side chain is located. It should be noted that no hydrogen bond between the guanidinium group and the backbone exists in the only $\gamma_L$[d] minimum characterized for this compound.

Table 3 reports the free energies in the gas phase ($\Delta G^{gp}$) at 298 K for the Ac-*t*-($^{\beta}$Pro)Arg-NHMe and Ac-*c*-($^{\beta}$Pro)Arg-NHMe minima described above. Consideration of the ZPVE, thermal, and entropic corrections to transform $\Delta E^{gp}$ into $\Delta G^{gp}$ affects substantially the relative energy order of the minimum-energy conformations characterized for the *trans*-($^{\beta}$Pro)Arg derivative. Specifically, $\alpha_L$[u]s$^-$g$^+$t becomes the most stable conformer, with $\gamma_L$[u]s$^-$g$^+$t being destabilized by 0.9 kcal/mol. Regarding the cis isomer, the relative stability of the

**Table 3.** Relative Free Energies[a] in the Gas Phase ($\Delta G^{gp}$) and in Carbon Tetrachloride, Chloroform and Aqueous Solutions ($\Delta G^{CCl_4}$, $\Delta G^{CHCl_3}$, and $\Delta G^{H_2O}$, respectively) at 298 K for Selected[b] Minimum-Energy Conformers of Ac-*t*-($^{\beta}$Pro)Arg-NHMe and Ac-*c*-($^{\beta}$Pro)Arg-NHMe at the B3LYP/6-31+G(d,p) Level

| conformer | $\Delta G^{gp}$ | $\Delta G^{CCl_4}$ | $\Delta G^{CHCl_3}$ | $\Delta G^{H_2O}$ |
|---|---|---|---|---|
| | Ac-*t*-($^{\beta}$Pro)Arg-NHMe | | | |
| $\gamma_L$[u]s$^-$g$^+$t | 0.9 | 1.2 | 2.5 | 6.5 |
| $\gamma_L$[u]g$^-$g$^-$s$^+$ | 2.6 | 0.6 | 0.3 | 2.6 |
| $\gamma_L$[u]g$^-$g$^-$s$^-$ | 2.0 | 1.5 | 1.9 | 4.9 |
| $\alpha_L$[u]s$^-$g$^+$t | 0.0[c] | 0.0 | 0.5 | 2.7 |
| $\alpha_L$[u]g$^+$g$^-$t | 3.1 | 3.2 | 3.6 | 4.9 |
| $\alpha_L$[u]g$^-$tg$^-$ | 4.1 | 1.2 | 0.0 | 0.0 |
| $\gamma_L$[u]s$^-$tg$^-$ | 5.1 | 2.4 | 1.9 | 4.2 |
| | Ac-*c*-($^{\beta}$Pro)Arg-NHMe | | | |
| $\alpha_L$[d]g$^+$g$^-$t | 0.0[d] | 0.0 | 1.1 | 2.1 |
| $\alpha_L$[d]g$^+$ts$^+$ | 3.0 | 0.2 | 0.0 | 0.0 |
| $\gamma_L$[d]s$^-$g$^+$t | 3.9 | 4.4 | 6.5 | 9.4 |
| $\gamma_L$[d]s$^-$ts$^-$ | 5.9 | 3.6 | 4.1 | 5.7 |
| $\gamma_L$[u]s$^+$g$^-$t | 5.8 | 6.0 | 7.9 | 10.2 |

[a] In kcal/mol. [b] Those given in Tables 1 and 2 ($\Delta E^{gp} < 5.0$ kcal/mol). [c] $G = -856.257478$ au. [d] $G = -856.256685$ au.

$\alpha_L$[d]g$^+$g$^-$t minimum is enhanced upon addition of these statistical contributions. The $\Delta G^{gp}$ values in Table 3 therefore indicate that $\alpha_L$ is the preferred backbone arrangement for both compounds in the gas phase. Assuming a Boltzmann distribution, the populations of $\alpha_L$ conformers at room temperature are about 80% and 100% for the trans and cis compounds, respectively. In contrast, minima of the $\gamma_L$ type showed the lowest $\Delta G^{gp}$ value for both Ac-*c*-($^{\gamma}$Pro)Arg-NHMe[28] and Ac-Pro-NHMe,[36] thus indicating a substantially higher tendency to adopt conformations in the $\alpha_L$ region for the arginine surrogates investigated in the present work, especially the cis isomer.

The effect of solvation was evaluated next by performing single-point calculations on the optimized structures through the PCM method. The presence of chlorinated solvents results in the stabilization of several Ac-*t*-($^{\beta}$Pro)Arg-NHMe minima (Table 3), in particular, $\gamma_L$[u]g$^-$g$^-$s$^+$ and $\alpha_L$[u]g$^-$tg$^-$. The relative stability of the latter notably increases with the polarity of the solvent. Indeed, it becomes the preferred structure in chloroform, even if two other minima exhibit relative free energies within a 0.5 kcal/mol interval, and it is the only accessible conformation at room temperature in aqueous solution. Regarding Ac-*c*-($^{\beta}$Pro)Arg-NHMe, only $\alpha_L$ structures are predicted to be populated either in the gas phase or in the different solvents considered (Table 3). For this compound, solvation seems to affect mainly the arrangement of the exocyclic substituent, with the g$^+$ts$^+$ disposition being favored with increasing polarity. Accordingly, $\alpha_L$[d]g$^+$ts$^+$ becomes the preferred conformation in chloroform and, to a larger extent, in aqueous solution.

Comparison of the solvation effects described above with those observed before[28] for the $\gamma$-substituted compound Ac-*c*-($^{\gamma}$Pro)Arg-NHMe provides further evidence for the higher stability of the $\alpha_L$ conformation in the arginine surrogates investigated in the present work. Indeed, minima of the $\gamma_L$ type showed the lowest $\Delta G$ value for the *cis*-($^{\gamma}$Pro)Arg derivative not only in the gas phase but also in carbon tetrachloride and chloroform solutions.[28] In water, conformations devoid of intramolecular hydrogen bonds between the backbone amide groups are usually favored for small peptides

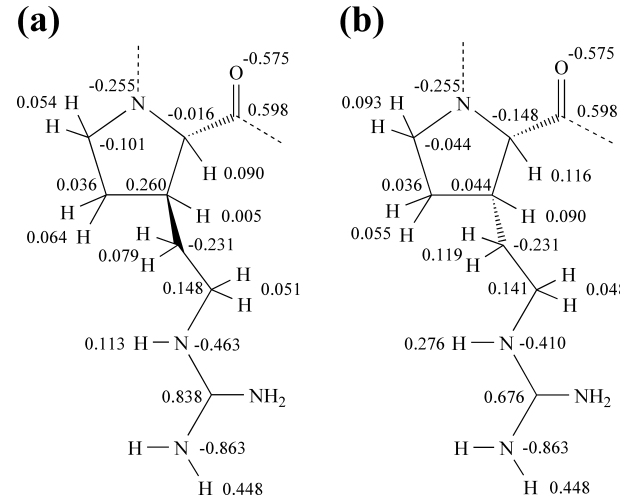


**Figure 5.** Electrostatic parameters determined for the (a) *trans*-($^{\beta}$Pro)Arg and (b) *cis*-($^{\beta}$Pro)Arg residues.

such as the ones considered here, and accordingly, an $\varepsilon_L$ conformer became the most populated structure for Ac-*c*-($^{\gamma}$Pro)Arg-NHMe in this solvent.[28] Interestingly, Ac-Pro-NHMe was predicted[36] to prefer the α-helical structure in water. The latter point shows that the conformational preferences of proline in aqueous solution are retained to a larger extent when the arginine side chain is attached to the $\beta$ position of the pyrrolidine moiety.

As stated in the Introduction, *trans*-($^{\beta}$Pro)Arg and *cis*-($^{\beta}$Pro)Arg are conceived as arginine substitutes in biologically active peptides. The conformational consequences arising from the incorporation of these arginine surrogates into such peptides can be analyzed by methods such as molecular dynamics (MD) simulations. For this purpose, previous parametrization of the nonproteinogenic residues is necessary. A specific set of force-field parameters was developed for *trans*-($^{\beta}$Pro)Arg and *cis*-($^{\beta}$Pro)Arg to describe the inter- and intramolecular interactions within the classical formalism. Our previous work showed that there is no special electronic effect that might condition the conformational preferences of proline upon addition of the arginine side chain,[28] and therefore, the stretching, bending, torsional, and van der Waals parameters for *trans*-($^{\beta}$Pro)Arg and *cis*-($^{\beta}$Pro)Arg were transferred directly from the AMBER force field.[41] Accordingly, electrostatic charges were the only force-field parameters specifically developed for these nonproteinogenic residues.

Atomic charges were calculated by fitting the HF/6-31G(d) quantum mechanical and Coulombic MEPs to a large set of points placed outside the nuclear region. The electrostatic parameters were obtained by weighting the charges calculated for the low-energy conformers of each compound according to a Boltzmann distribution.[42−45] The latter was estimated with the $\Delta G^{gp}$ values listed in Table 3. The $\alpha_L$[u]s$^-$g$^+$t, $\gamma_L$[u]s$^-$g$^+$t, and $\gamma_L$[u]g$^-$g$^-$s$^-$ structures were considered for the trans isomer, whereas $\alpha_L$[d]g$^+$g$^-$t was the only conformer used for the cis derivative because all of the local minima are destabilized by at least 3.0 kcal/mol. The electrostatic parameters obtained for *trans*-($^{\beta}$Pro)Arg and *cis*-($^{\beta}$Pro)Arg are given in Figure 5.

To check the validity of classical MD simulations in describing the conformational properties of the arginine analogues under study, MD with explicit solvent molecules

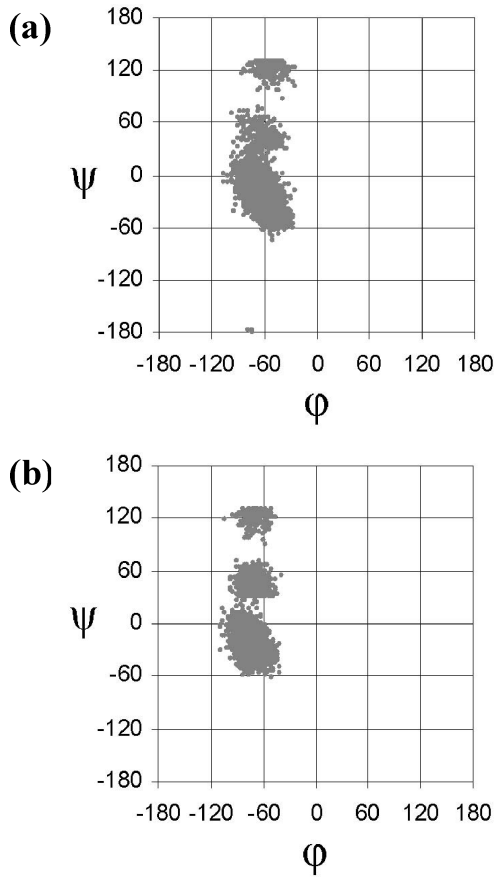


**Figure 6.** Accumulated Ramachandran plots for (a) Ac-*t*-($^{\beta}$Pro)Arg-NHMe and (b) Ac-*c*-($^{\beta}$Pro)Arg-NHMe derived from MD simulations in aqueous solution.

was performed on Ac-*t*-($^{\beta}$Pro)Arg-NHMe and Ac-*c*-($^{\beta}$Pro)Arg-NHMe in aqueous solution at 298 K. For each compound, the lowest-energy conformation was used as the starting point of a 10-ns trajectory. Figure 6 presents the accumulated Ramachandran plot obtained for each derivative. In both cases, the most populated backbone structure corresponds to $\alpha_L$, which is visited much more frequently than the $\gamma_L$ region during the trajectory. This finding is in excellent agreement with the results reported in Table 3, which indicate that $\alpha_L$ is the most favored conformation in aqueous solution for both compounds.

## CONCLUSIONS

Two isomers of an arginine surrogate have been built by attaching the arginine side chain to the proline $\beta$-carbon in either a *trans* or a *cis* disposition relative to the carboxylic acid. The resulting amino acids, denoted *trans*-($^{\beta}$Pro)Arg and *cis*-($^{\beta}$Pro)Arg, respectively, combine the conformational restrictions associated with the cyclic nature of proline with the side-chain functionality of arginine. Quantum mechanics calculations on the *N*-acetyl-*N*′-methylamide derivatives of these arginine surrogates show that the conformational space available is highly restricted, as expected from their proline-like character. Their conformational preferences are essentially determined by their cyclic structure and the capacity of the guanidilated side chain to establish hydrogen-bonding interactions with the peptide backbone. The latter factor is especially significant for the $\alpha_L$ conformation, which is stabilized with respect to natural proline[36] and is predicted to be the most populated structure for both ($^{\beta}$Pro)Arg isomers not only in the gas phase but also in aqueous solution. MD simulations show that the restricted flexibility and the preference for α-helical conformations are kept when thermal agitation is included.

The two noncoded amino acids studied in the present work are suitable candidates to replace arginine in bioactive peptides when the natural residue is found in the $\alpha_L$ region, and more specifically, occupying the $i + 1$ position of a $\beta$-turn of type I. In particular, *cis*-($^{\beta}$Pro)Arg might be an excellent replacement for arginine in CREKA and more appropriate than the arginine surrogate considered in a previous work.[28] Thus, *cis*-($^{\beta}$Pro)Arg is expected not only to increase resistance to proteases but also to greatly stabilize the type I $\beta$-turn found in CREKA. For other biologically relevant peptides, either the cis or the trans isomer of ($^{\beta}$Pro)Arg might be adequate to replace arginine depending on the orientation attained by the guanidilated side chain in the bioactive conformation.

## ACKNOWLEDGMENT

Gratitude is expressed to the Centre de Supercomputació de Catalunya (CESCA). We also acknowledge the National Cancer Institute for partial allocation of computing time and staff support at the Advanced Biomedical Computing Center of the Frederick Cancer Research and Development Center. Classical calculations were partially carried out using the high-performance computational capabilities of the Biowulf PC/Linux cluster at the National Institutes of Health, Bethesda, MD (http://biowulf.nih.gov). Financial support from the Ministerio de Educación y Ciencia (Ramon y Cajal contract for D.Z., Project CTQ2007-62245), Gobierno de Aragón (research group E40), and Generalitat de Catalunya (research group 2009 SGR 925; XRQTC; ICREA Academia prize for excellence in research to C.A.) is gratefully acknowledged. This project has been funded in whole or in part with federal funds from the National Cancer Institute, National Institutes of Health, under Contract HHSN261200-800001E. The content of this publication does not necessarily reflect the view of the policies of the Department of Health and Human Services, nor does mention of trade names, commercial products, or organizations imply endorsement by the U.S. Government. This research was supported (in part) by the Intramural Research Program of the NIH, National Cancer Institute, Center for Cancer Research.

**Supporting Information Available:** All minimum-energy conformations characterized for Ac-*t*-($^{\beta}$Pro)Arg-NHMe and Ac-*c*-($^{\beta}$Pro)Arg-NHMe at the B3LYP/6-31+G(d,p) level. Some methodological details about the design of the noncoded amino acids studied. This material is available free of charge via the Internet at http://pubs.acs.org.

## REFERENCES AND NOTES

(1) Venkatraman, J.; Shankaramma, S. C.; Balaram, P. Design of Folded Peptides. *Chem. Rev.* **2001**, *101*, 3131–3152.
(2) Toniolo, C.; Crisma, M.; Formaggio, F.; Peggion, C. Control of Peptide Conformation by the Thorpe−Ingold Effect ($C^{\alpha}$-Tetrasubstitution). *Biopolymers (Pept. Sci.)* **2001**, *60*, 396–419.
(3) Nestor, J. J. The Medicinal Chemistry of Peptides. *Curr. Med. Chem.* **2009**, *16*, 4399–4418.
(4) Horne, W. S.; Gellman, S. H. Foldamers with Heterogeneous Backbones. *Acc. Chem. Res.* **2008**, *41*, 1399–1408.

(5) Chatterjee, J.; Gilon, C.; Hoffman, A.; Kessler, H. N-Methylation of Peptides: A New Perspective in Medicinal Chemistry. *Acc. Chem. Res.* **2008**, *41*, 1331–1342.
(6) Lelais, G.; Seebach, D. $\beta^2$-Amino Acids−Syntheses, Occurrence in Natural Products, and Components of $\beta$-Peptides. *Biopolymers (Pept. Sci.)* **2004**, *76*, 206–243.
(7) Adessi, C.; Soto, C. Converting a Peptide into a Drug: Strategies to Improve Stability and Bioavailability. *Curr. Med. Chem.* **2002**, *9*, 963–978.
(8) *Peptide and Protein Design for Biopharmaceutical Applications*; Jensen, K. J., Ed.; John Wiley & Sons: Chichester, U.K., 2009.
(9) *Pseudo-Peptides in Drug Discovery*; Nielsen, P. E., Ed.; Wiley-VCH: Weinheim, Germany, 2004.
(10) Simberg, D.; Duza, T.; Park, J. H.; Essler, M.; Pilch, J.; Zhang, L.; Derfus, A. M.; Yang, M.; Hoffman, R. M.; Bathia, S.; Sailor, M. J.; Ruoslahti, E. Biomimetic Amplification of Nanoparticle Homing to Tumors. *Proc. Natl. Acad. Sci. U.S.A.* **2007**, *104*, 932–936.
(11) Zanuy, D.; Flores-Ortega, A.; Casanovas, J.; Curcó, D.; Nussinov, R.; Alemán, C. The Energy Landscape of a Selective Tumor-Homing Pentapeptide. *J. Phys. Chem. B* **2008**, *112*, 8692–8700.
(12) Agemy, L.; Sugahara, K. N.; Kotamraju, V. R.; Gujraty, K.; Girard, O. M.; Kono, Y.; Mattrey, R. F.; Park, J. H.; Sailor, M. J.; Jimenez, A. I.; Cativiela, C.; Zanuy, D.; Sayago, F. J.; Aleman, C.; Nussinov, R.; Ruoslahti, E. Nanoparticle-induced vascular blockade in human prostate cancer. *Blood*, published online Jun 29, 2010, http://dx.doi.org+10.1182/blood-2010-03-274258.
(13) Revilla-Lopez, G.; Torras, J.; Jimenez, A. I.; Cativiela, C.; Nussinov, R.; Aleman, C. Side-Chain to Backbone Interactions Dictate the Conformational Preferences of a Cyclopentane Arginine Analogue. *J. Org. Chem.* **2009**, *74*, 2403–2412.
(14) Alemán, C. Conformational properties of α-amino acids disubstituted at the α-carbon. *J. Phys. Chem. B* **1997**, *101*, 5046–5050.
(15) Alemán, C.; Jiménez, A. I.; Cativiela, C.; Perez, J. J.; Casanovas, J. Influence of the phenyl side chain on the conformation of cyclopropane analogues of phenylalanine. *J. Phys. Chem. B* **2002**, *106*, 11849–11858.
(16) Casanovas, J.; Zanuy, D.; Nussinov, R.; Alemán, C. Identification of the intrinsic conformational properties of 1-aminocyclobutane-1-carboxylic acid. *Chem. Phys. Lett.* **2006**, *429*, 558–562.
(17) Alemán, C.; Zanuy, D.; Casanovas, J.; Cativiela, C.; Nussinov, R. Backbone Conformational Preferences and Pseudorotational Ring Puckering of 1-Aminocyclopentane-1-carboxylic Acid. *J. Phys. Chem. B* **2006**, *110*, 21264–21271.
(18) Rodriguez-Ropero, F.; Zanuy, D.; Casanovas, J.; Nussinov, R. Alemán, C Application of 1-Aminocyclohexane Carboxylic Acid to Protein Nanostructure Computer Design. *J. Chem. Inf. Model.* **2008**, *48*, 333–343.
(19) Markert, Y.; Köditz, J.; Ulbrich-Hofmann, R.; Arnold, U. Proline versus Charge Concept for Protein Stabilization against Proteolytic Attack. *Protein Eng.* **2003**, *16*, 1041–1046.
(20) Walker, J. R.; Altman, R. K.; Warren, J. W.; Altman, E. Using Protein-Based Motifs to Stabilize Peptides. *J. Pept. Res.* **2003**, *62*, 214–226.
(21) Vanhoof, G.; Goossens, F.; De Meester, I.; Hendriks, D.; Scharpé, S. Proline Motifs in Peptides and Their Biological Processing. *FASEB J.* **1995**, *9*, 736–744.
(22) Frenken, L. G. J.; Egmond, M. R.; Batenburg, A. M.; Verrips, C. T. *Pseudomonas glumae* lipase: Increased proteolytic stability by protein engineering. *Protein Eng.* **1993**, *6*, 637–642.
(23) Chakrabarti, P.; Pal, D. The Interrelationships of Side-Chain and Main-Chain Conformations in Proteins. *Prog. Biophys. Mol. Biol.* **2001**, *76*, 1–102.
(24) MacArthur, M. W.; Thornton, J. M. Influence of Proline Residues on Protein Conformation. *J. Mol. Biol.* **1991**, *218*, 397–412.
(25) Rose, G. D.; Gierasch, L. M.; Smith, J. A. Turns in Peptides and Proteins. *Adv. Protein Chem.* **1985**, *37*, 1–109.
(26) Che, Y.; Marshall, G. R. Impact of *Cis*-Proline Analogues on Peptide Conformation. *Biopolymers* **2006**, *81*, 392–406.
(27) Sahai, M. A.; Fejer, S. N.; Viskolcz, B.; Pai, E. F.; Csizmadia, I. G. First-Principles Computational Study on the Full Conformational Space of L-Threonine Diamide, the Energetic Stability of Cis and Trans Isomers. *J. Phys. Chem. A* **2006**, *110*, 11527–11536.
(28) Zanuy, D.; Flores-Ortega, A.; Jiménez, A. I.; Calaza, M. I.; Cativiela, C.; Nussinov, R.; Ruoslahti, E.; Alemán, C. In Silico Molecular Engineering for a Targeted Replacement in a Tumor-Homing Peptide. *J. Phys. Chem. B* **2009**, *113*, 7879–7889.
(29) Frisch, M. J.; Trucks, G. W.; Schlegel, H. B.; Scuseria, G. E.; Robb, M. A.; Cheeseman, J. R.; Montgomery, J. A., Jr.; Vreven, T.; Kudin, K. N.; Burant, J. C.; Millam, J. M.; Iyengar, S. S.; Tomasi, J.; Barone, V.; Mennucci, B.; Cossi, M.; Scalmani, G.; Rega, N.; Petersson, G. A.; Nakatsuji, H.; Hada, M.; Ehara, M.; Toyota, K.; Fukuda, R.; Hasegawa, J.; Ishida, M.; Nakajima, T.; Honda, Y.; Kitao, O.; Nakai, H.; Klene, M.; Li, X.; Knox, J. E.; Hratchian, H. P.; Cross, J. B.; Bakken, V.; Adamo, C.; Jaramillo, J.; Gomperts, R.; Stratmann, R. E.; Yazyev, O.; Austin, A. J.; Cammi, R.; Pomelli, C.; Ochterski, J. W.; Ayala, P. Y.; Morokuma, K.; Voth, G. A.; Salvador, P.; Dannenberg, J. J.; Zakrzewski, V. G.; Dapprich, S.; Daniels, A. D.; Strain, M. C.; Farkas, O.; Malick, D. K.; Rabuck, A. D.; Raghavachari, K.; Foresman, J. B.; Ortiz, J. V.; Cui, Q.; Baboul, A. G.; Clifford, S.; Cioslowski, J.; Stefanov, B. B.; Liu, G.; Liashenko, A.; Piskorz, P.; Komaromi, I.; Martin, R. L.; Fox, D. J.; Keith, T.; Al-Laham, M. A.; Peng, C. Y.; Nanayakkara, A.; Challacombe, M.; Gill, P. M. W.; Johnson, B.; Chen, W.; Wong, M. W.; Gonzalez, C.; Pople, J. A. *Gaussian 03*, revision B.02; Gaussian, Inc.: Pittsburgh, PA, 2003.
(30) Becke, A. D. A New Mixing of Hartree−Fock and Local Density-Functional Theories. *J. Chem. Phys.* **1993**, *98*, 1372–1377.
(31) Lee, C.; Yang, W.; Parr, R. G. Development of the Colle−Salvetti Correlation-Energy Formula into a Functional of the Electron-Density. *Phys. Rev. B* **1988**, *37*, 785–789.
(32) McLean, A. D.; Chandler, G. S. Contracted Gaussian Basis Sets for Molecular Calculations. I. Second Row Atoms, $Z = 11-18$. *J. Chem. Phys.* **1980**, *72*, 5639−5648.
(33) Perczel, A.; Angyán, J. G.; Kajtar, M.; Viviani, W.; Rivail, J.-L.; Marcoccia, J.-F.; Csizmadia, I. G. Peptide Models. 1. Topology of Selected Peptide Conformational Potential Energy Surfaces (Glycine and Alanine Derivatives). *J. Am. Chem. Soc.* **1991**, *113*, 6256–6265.
(34) Milner-White, E. J.; Bell, L. H.; Maccallum, P. H. Pyrrolidine Ring Puckering in *cis* and *trans*-Proline Residues in Proteins and Polypeptides−Different Puckers are Favoured in Certain Situations. *J. Mol. Biol.* **1992**, *228*, 725–734.
(35) Némethy, G.; Gibson, K. D.; Palmer, K. A.; Yoon, C. N.; Paterlini, G.; Zagari, A.; Rumsey, S.; Scheraga, H. A. Energy Parameters in Polypeptides. 10. Improved Geometrical Parameters and Nonbonded Interactions for Use in the ECEPP/3 Algorithm, with Application to Proline-Containing Peptides. *J. Phys. Chem.* **1992**, *96*, 6472–6484.
(36) Flores-Ortega, A.; Jiménez, A. I.; Cativiela, C.; Nussinov, R.; Alemán, C.; Casanovas, J. Conformational Preferences of α-Substituted Proline Analogues. *J. Org. Chem.* **2008**, *73*, 3418–3427.
(37) Tomasi, J.; Mennucci, B.; Cammi, R. Quantum Mechanical Continuum Solvation Models. *Chem. Rev.* **2005**, *105*, 2999–3093.
(38) Tomasi, J.; Persico, M. Molecular Interactions in Solution: An Overview of Methods Based on Continuous Distributions of the Solvent. *Chem. Rev.* **1994**, *94*, 2027–2094.
(39) Miertus, S.; Tomasi, J. Approximate Evaluations of the Electrostatic Free Energy and Internal Energy Changes in Solution Processes. *Chem. Phys.* **1982**, *65*, 239–245.
(40) Miertus, M.; Scrocco, E.; Tomasi, J. Electrostatic Interaction of a Solute with a Continuum. A Direct Utilization of Ab Initio Molecular Potentials for the Prevision of Solvent Effects. *Chem. Phys.* **1981**, *55*, 117–129.
(41) Cornell, W. D.; Cieplak, P.; Bayly, C. I.; Gould, I. R.; Merz, K. M.; Ferguson, D. M.; Spellmeyer, D. C.; Fox, T.; Caldwell, J. W.; Kollman, P. A. A Second Generation Force Field for the Simulation of Proteins, Nucleic Acids, and Organic Molecules. *J. Am. Chem. Soc.* **1995**, *117*, 5179–5197.
(42) Cieplak, P.; Cornell, W. D.; Bayly, C.; Kollman, P. A. Application of the Multimolecule and Multiconformational RESP Methodology to Biopolymers: Charge Derivation for DNA, RNA, and Proteins. *J. Comput. Chem.* **1995**, *16*, 1357−1377.
(43) Alemán, C.; Casanovas, J. Ab Initio SCF and Force-Field Calculations on Low-Energy Conformers of 2-Acetylamino-2,*N*-Dimetylpropanamide. *J. Chem. Soc., Perkin Trans. 2* **1994**, 563–568.
(44) Reynolds, C. A.; Essex, J. W.; Richards, W. G. Atomic Charges for Variable Molecular Conformations. *J. Am. Chem. Soc.* **1992**, *114*, 9075–9079.
(45) Casanovas, J.; Zanuy, D.; Nussinov, R.; Alemán, C. Intrinsic Conformational Characteristics of α,α-Diphenylglycine. *J. Org. Chem.* **2007**, *72*, 2174–2181.
(46) Kalé, L.; Skeel, R.; Bhandarkar, M.; Brunner, R.; Gursoy, A.; Krawetz, N.; Phillips, J.; Shinozaki, A.; Varadarajan, K.; Schulten, K. NAMD2: Greater Scalability for Parallel Molecular Dynamics. *J. Comput. Phys.* **1999**, *151*, 283–312.
(47) Jorgensen, W. L.; Chandrasekhar, J.; Madura, J. D.; Impey, R. W.; Klein, M. L. Comparison of Simple Potential Functions for Simulating Liquid Water. *J. Chem. Phys.* **1983**, *79*, 926–935.
(48) Berendsen, H. J. C.; Postma, J. P. M.; van Gunsteren, W. F.; DiNola, A.; Haak, J. R. Molecular Dynamics with Coupling to an External Bath. *J. Chem. Phys.* **1984**, *81*, 3684–3690.
(49) Ryckaert, J. P.; Ciccotti, G.; Berendsen, H. J. C. Numerical Integration of the Cartesian Equations of Motion of a System with Constraints: Molecular Dynamics of *n*-Alkanes. *J. Comput. Phys.* **1977**, *23*, 327–341.

CI100135F